THE JOURNAL OF PHYSICAL CHEMISTRY B

Article

pubs.acs.org/JPCB

Thermodynamics, Kinetics, and Photochromism of Oaklins: A Recent Family of Deoxyanthocyanidins

André Sousa,[†] Vesselin Petrov,[‡] Paula Araújo,[†] Nuno Mateus,[†] Fernando Pina,*[,‡] and Victor de Freitas*[,†]

[†]Centro de Investigação em Química, Departamento de Química, Faculdade de Ciências, Universidade do Porto, Rua do Campo Alegre, 687, 4169-007 Porto, Portugal

[‡]REQUIMTE, Departamento de Química, Faculdade de Ciências e Tecnologia, Universidade Nova de Lisboa, 2829-516 Caparica, Portugal

ABSTRACT: Two oaklins guaiacylcatechinpyrylium (GCP) and syringylcatechinpyrylium (SCP) and a model compound deoxypeonidin (DOP) were synthesized, and the rate and equilibrium constants of the respective pH dependent network of chemical reactions were calculated. In contrast to anthocyanins, the three compounds possess a small *cis*−*trans* isomerization barrier and hence the rate of the *trans*-chalcone formation follows a bell-shaped curve as a function of pH. The three compounds exhibit photochromism obtained by irradiation of the *trans*-chalcone, which, depending on pH, leads to the colored species flavylium cation and quinoidal base. The flash photolysis together with pH jumps followed by UV−vis absorption and stopped flow is a very useful tool to achieve the rate and equilibrium constants of the network of chemical reactions followed by these molecules. Oaklin compounds which are formed in wine aged in oak barrels present physical-chemical properties more similar to simpler deoxyanthocyanidins rather than anthocyanins and may play a significant role in color changes observed in wine aging. Given their higher stability, they may be regarded as potential food colorants.

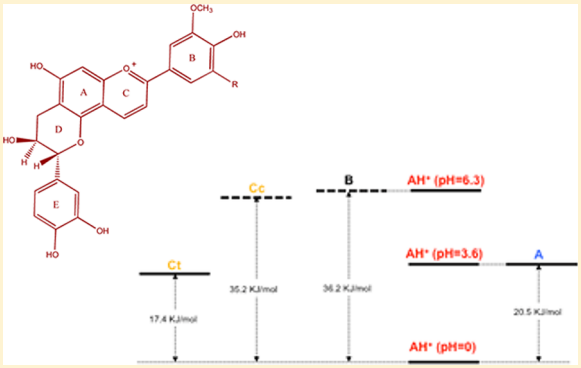

INTRODUCTION

2-Phenyl-1-benzopyrilium (flavylium) derivatives, which comprise anthocyanins, deoxyanthocyanins, anthocyanidins, as well as bioinspired synthetic flavylium compounds, have been a recurrent subject of research through more than a century.[1] This is due to the role played by anthocyanins as colorants of most flowers and fruits and to the antioxidant properties of these compounds and the consequent potential of their applications in human health.[2]

In general, independently of their natural or synthetic origin, flavylium derivatives follow the same network of chemical reactions as reported in Scheme 1 for malvidin-3-glucoside.

Despite the apparent complexity of the pH dependent chemistry of flavylium compounds, due to the manifold of chemical reactions involving these compounds, the system can be viewed as a single acid−base equilibrium involving flavylium cation and its conjugate base **CB**, eq 1

$$\mathbf{AH}^+ + H_2O \rightleftharpoons \mathbf{CB} + H_3O^+ \qquad K'_a = K_a + K_h + K_hK_t + K_hK_tK_i \tag{1}$$

CB is defined as the sum of the concentrations of the other species in the network, [CB] = [A] + [B] + [Cc] + [Ct].[3−7]

The global equilibrium defined by eq 1 is decomposed in their components according to eqs 2−5.

$\mathbf{AH}^+ + H_2O \rightleftharpoons \mathbf{A} + H_3O^+$	K_a	Proton transfer	(2)
$\mathbf{AH}^+ + 2H_2O \rightleftharpoons \mathbf{B} + H_3O^+$	K_h	Hydration	(3)
$\mathbf{B} \rightleftharpoons \mathbf{Cc}$	K_t	Tautomerization	(4)
$\mathbf{Cc} \rightleftharpoons \mathbf{Ct}$	K_i	Isomerization	(5)

The percentage of each of the "basic species of CB" is dramatically dependent on the substitution pattern of the flavylium core. For example, in anthocyanins, **B** is the major species, while, in 7,4′-dihydroxyflavylium, it is the *trans*-chalcone **Ct**.[1,8] It is worth noting the reversibility of all the reactions, at least in acidic medium, which makes the flavylium network a unique multicomponent system. Photochemistry takes place upon irradiation of **Ct**, leading to **Cc**, which spontaneously gives flavylium cation and/or quinoidal base depending on pH. The photochemical system is reversible, and **Ct** is recovered through the thermal back reaction.

In this work, the compounds guaiacylcathechinpyrylium (GCP), syringylcatechinpyrylium (SCP), and the model compound deoxypeonidin (DOP) (Scheme 2) were synthesized and the thermodynamics and the kinetics of the respective network fully described.

Received: November 7, 2012
Revised: January 14, 2013
Published: January 15, 2013

   dx.doi.org/10.1021/jp3110216 | *J. Phys. Chem. B* 2013, 117, 1901−1910

Scheme 1. Network of Chemical Reactions of Malvidin-3-glucoside

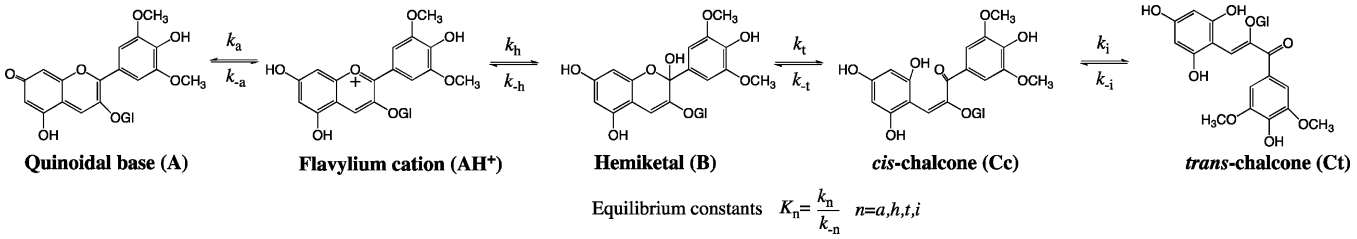

Scheme 2. The Model Compound Deoxypeonidin (DOP) and the Derivatives Guaiacylcathechinpyrylium (GCP) and Syringylcatechinpyrylium (SCP)

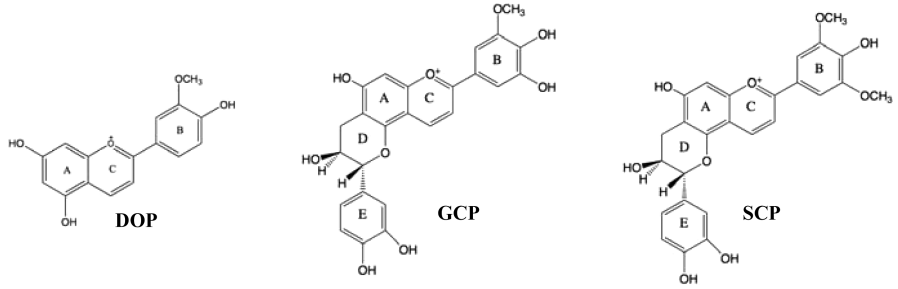

The formation and synthesis of the catechinpyrylium compounds SCP and GCP was previously described and these compounds named oaklins, a new class of brick-red colored pigments resulting from the reaction between catechin and wood aldehydes.[9,10] The formation of these pigments was also performed in a wine model solution, and one of these (GCP) was also found in real wines aged in oak barrels, confirming that this type of compounds may contribute to the overall color changes observed during the aging process. Oppositely to anthocyanins, these pigments do not possess a glucose group in the flavylium core and are classified as deoxyanthocyanidins. To test and compare the properties of these compounds, a structurally simpler deoxyanthocyanidin (DOP) was also synthesized.

There is interest in knowing how the structural modifications carried out in the model compound DOP to give GCP and SCP affect the network of chemical reactions reported above, and in particular the photochromic properties, as well as to make an argument regarding the stability of these compounds and their putative role in color changes in wine aging when compared to common wine anthocyanins. Furthermore, deoxyanthocyanidins are reported to be much more stable in slightly acidic solutions than anthocyanins and anthocyanidins, which points to the potential advantage of this type of compounds as viable commercial food colorants, and justifies the research developed in the chemistry of 3-deoxyanthocyanins and, in particular, the search for new colorants with significant stability.[11−13]

EXPERIMENTAL SECTION

Synthesis of GCP (Guaiacylcatechinpyrylium), SCP (Syringylcatechinpyrylium), and DOP (Deoxypeonidin). Regarding the synthesis of GCP, catechin ((2*R*,3*S*)-2-(3,4-dihydroxyphenyl)-3,4-dihydro-2*H*-chromene-3,5,7-triol) (8 mM) was incubated with coniferaldehyde ((*E*)-3-(4-hydroxy-3-methoxyphenyl)prop-2-enal) (8 mM) in 100 mL of a 12% ethanol−water solution (v/v) at pH 1.5 at 35 °C. The formation of the compound was followed over time by HPLC−DAD using a reversed phase C-18 (Merck) column (250 × 4.6 mm i.d., particle size 5 μm) at 25 °C. Solvents were (A) water/formic acid (95:5) and (B) acetonitrile. The elution gradient was performed using an L-2130 Merck pump from 10 to 35% B for 55 min at a flow rate of 1.5 mL min^{-1}. When the reaction was completed, after 10 days, the sample was applied on a silica gel C-18 reversed phase SPE cartridge in order to remove inorganic salts and other impurities and the pigments were eluted with acidified methanol (2% v/v). Methanol was evaporated in a rotary evaporator at 38 °C, and the sample was freeze-dried and stored at −18 °C until use. The sample was further applied into a 5 cm diameter medium porosity sintered glass funnel with TSK Toyopearl gel HW-40(S) (Tosoh), connected to standard vacuum filtration glassware and gradually eluted with increasing percentages of acidified methanol (F1, 30%; F2, 40%; F3, 50%; F4, 60%; F5, 80%). The criterion used for changing the percentages of methanol was the decrease in color intensity of the solution eluted from the column. Semipreparative HPLC was performed in order to further isolate and purify the GCP compound, eluted in fraction F2 from Toyopearl gel. This fraction was injected into a reversed phase C-18 (Merck) column (250 × 4.6 mm i.d., particle size 5 μm) at room temperature (the volume injected was 1 mL). Solvents were (A) water/formic acid (95:5) and (B) acetonitrile. The elution gradient was performed using a L-2130 Elite LaChrom pump from 10 to 35% B for 65 min at a flow rate of 1.5 mL min^{-1}, and detection was carried out at 500 nm using a L-2420 Elite LaChrom detector. The synthesis of syringilcatechinpyrylium (SCP) was performed using the same procedure.

The synthesis of the compound 3-deoxypeonidin was followed according to the procedure described in ref 14. Phloroglucinol (8 mM) was incubated with coniferaldehyde (80 mM) in a 100 mL 12% ethanol−water solution (v/v) at pH 1.0 at 35 °C. When the reaction was completed, after 4 days, the sample was applied on a silica gel C-18 reversed phase SPE cartridge in order to remove inorganic salts and other impurities and the pigments were eluted with methanol acidulated with 2% HCl. The sample was further applied into a 300 × 16 mm i.d. TSK Toyopearl gel HW-40(S) (Tosoh, Japan) column and eluted with 40% aqueous methanol in 4 h.

UV/vis absorption spectra were recorded on a Varian Cary 100 Bio and Varian Cary 5000 spectrophotometers. The stopped flow experiments were conducted in an Applied Photophysics SX20 stopped-flow spectrometer provided with a PDA.1/UV photodiode array detector with a minimum scan time of 0.65 ms and a

dx.doi.org/10.1021/jp3110216 | J. Phys. Chem. B 2013, 117, 1901−1910

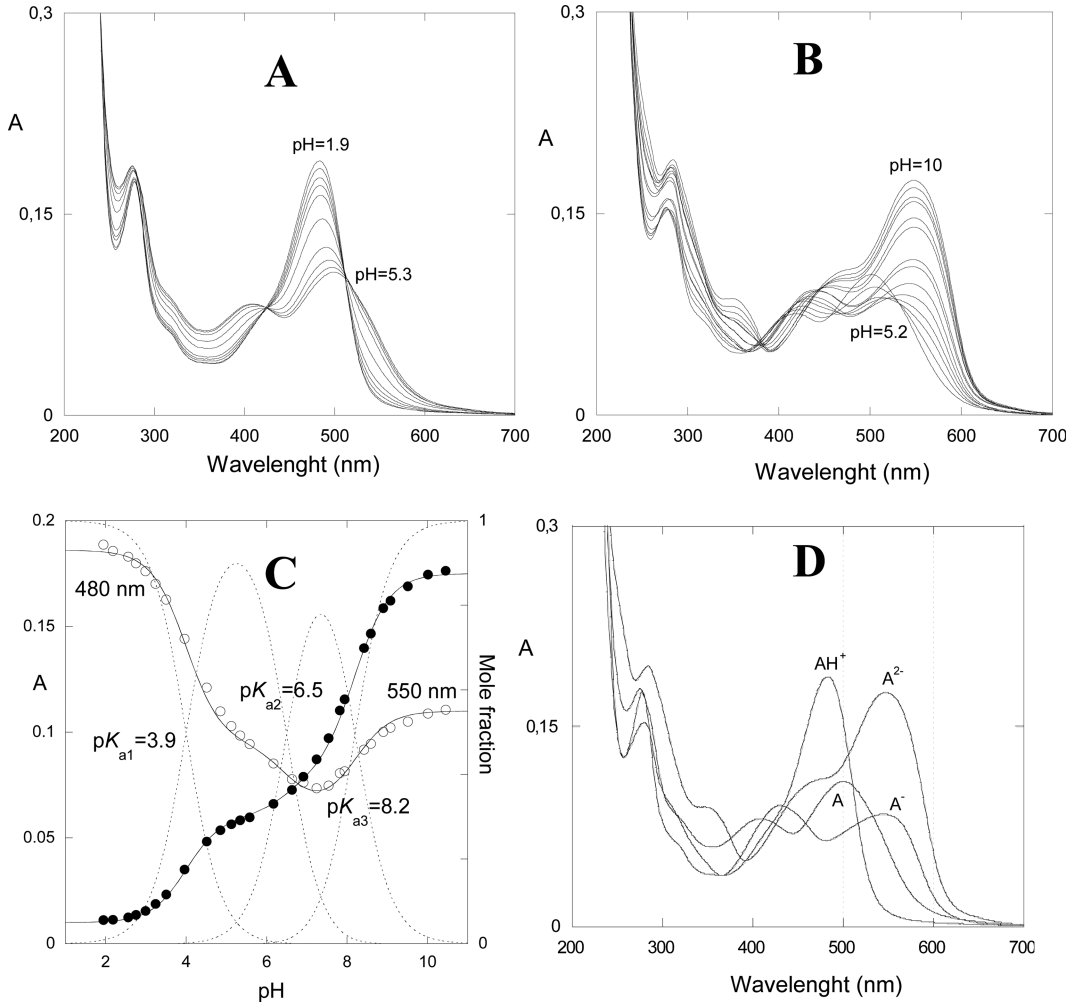

Figure 1. (A) Spectral variations of the compound deoxypeonidin immediately after a pH jump from 1 to the range 1.9 < pH < 5.3. (B) The same for 5.3 < pH < 10. (C) Fitting of the absorption at 480 and 550 nm as a function of pH. (D) Absorption spectra of the flavylium cation, quinoidal base, and ionized quinoidal bases obtained by mathematical decomposition.

Table 1. Ionization Constants of DOP, GCP, and SCP

compound	pK_{a1}	pK_{a2}	pK_{a3}
DOP	4.0 ± 0.1	6.5 ± 0.1	8.2 ± 0.1
GCP	3.6 ± 0.1	7.7 ± 0.1	
SCP	3.8 ± 0.1	n.d.[a]	

[a]n.d.: not determined.

wavelength range of 200−700 nm. Flash photolysis was carried out as reported elsewhere:[15] to monitor the transient species, a common spectrophotometer with a slightly modified compartment was used: (i) a slit (5 mm wide and 20 mm high) was opened on the external side of the sample holder in order to perform light excitation perpendicular to the analyzing beam; (ii) the whole sample compartment shielded (except for the slit described above) with black cardboard and black tape, to reduce as much as possible the flash light entering the exit slits. The time driven acquisition mode of the spectrophotometer was used, and the traces were obtained each 5 nm or less according to the accuracy needed. From the traces, the time dependent absorption spectra were calculated.

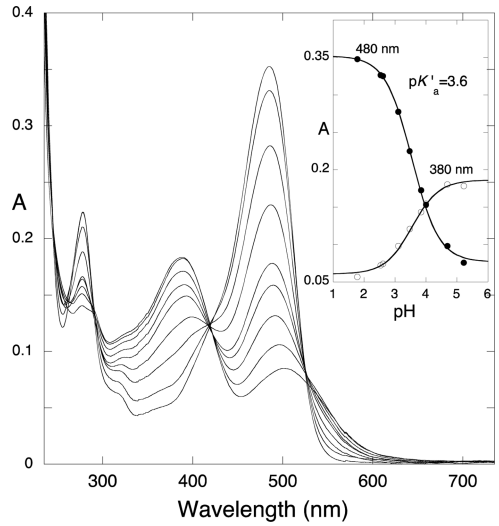

Figure 2. Spectra of equilibrated solutions of deoxypeonidin at different pH values, showing the equilibrium between AH^+, A, and Ct; inset representation of the fitting obtained at two different wavelengths (pK'_a = 3.6 ± 0.1).

RESULTS

1. Deoxypeonidin (DOP). Figure 1 shows the spectral variations of the model compound deoxypeonidin, 5,7,4′-trihydroxy-3′-methoxyflavylium (DOP), occurring immediately after a pH jump from stock solutions at pH 1 to higher pH values

dx.doi.org/10.1021/jp3110216 | J. Phys. Chem. B 2013, 117, 1901−1910

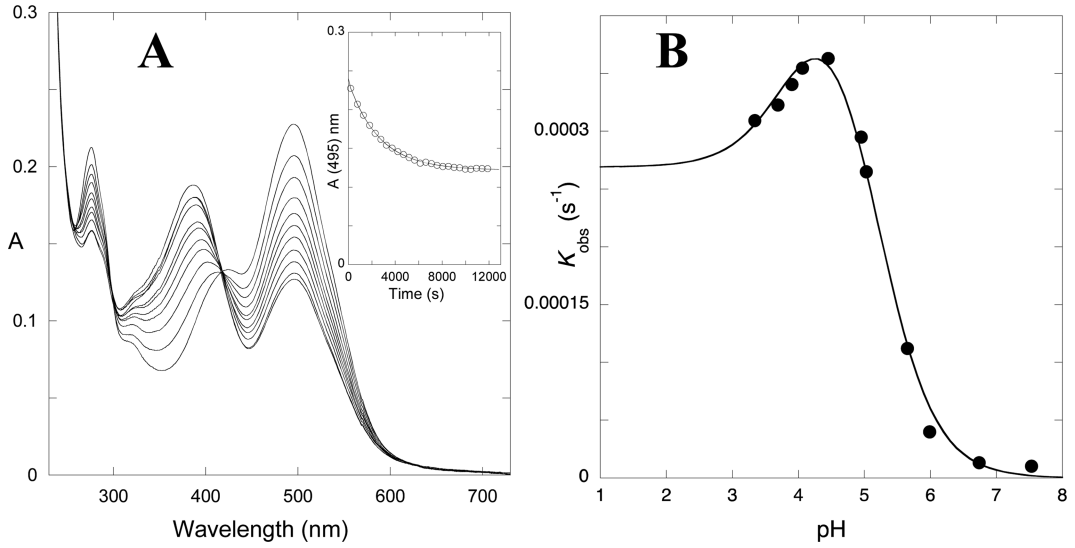

Figure 3. (A) Spectral variations after a pH jump from 1 to 4.7 (k_{obs} = 3.8 × 10^{-4} s^{-1}) - inset trace at 495 nm, the ratio between the final absorbance and initial one gives 0.54. (B) Representation of the observed rate constant as a function of pH. Fitting was achieved for pK_a = 3.9; $K_hK_tk_i$ = 2.6 × 10^{-8}; k_{-i} = 2.55 × 10^{-4} s^{-1}; k_iK_t/k_{-h} = 6.65 × 10^{-6} M.

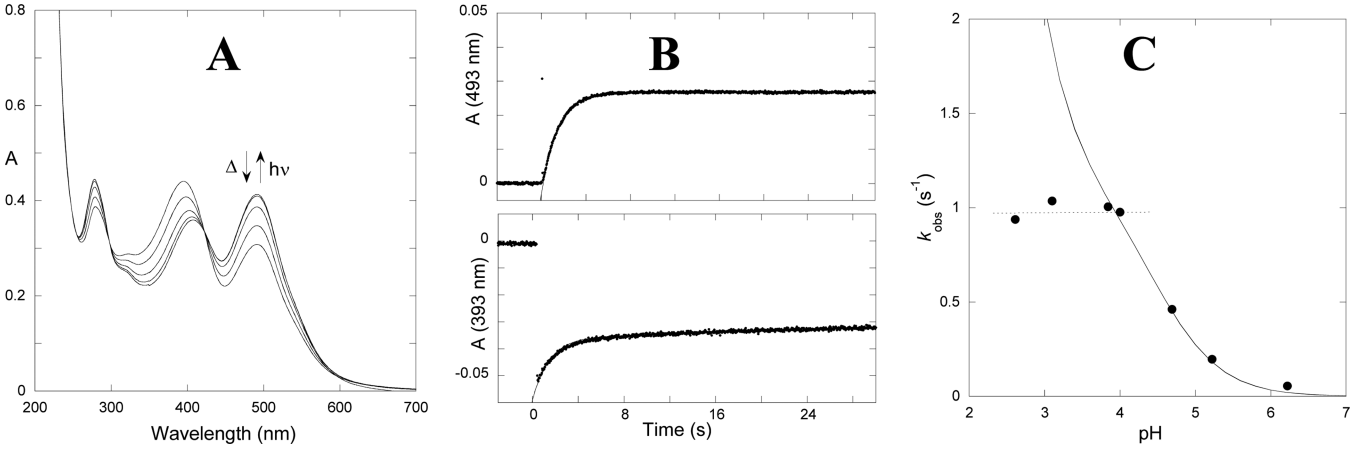

Figure 4. (A) Spectral variations following the irradiation of DOP at pH 4.3 at an irradiation wavelength of 366 nm. (B) Flash photolysis of a solution of DOP, pH 4.4: flash photolysis showing the trace of the flavylium formation (493 nm) up and the recovery of the *trans*-chalcone (393 nm) down. (C) Representation of the rate constants of the flash photolysis process as a function of pH.

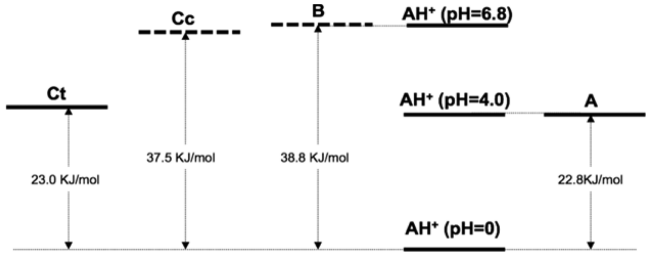

Figure 5. Energy level diagram for DOP based on the equilibrium constants of Table 1. The energy levels of B and Cc were obtained through the fitting of eqs 7−9 due to the lack of observation of traces corresponding to B and Cc in the reverse pH jump experiments carried out by stopped flow.

Table 2. Equilibrium Constants

compound	pK'_a	K_h[a] (M^{-1})	K_t[a]	K_i[a]
DOP	3.6 ± 0.1	1.7 × 10^{-7}	1.7	350
GCP	3.05 ± 0.1	4.6 × 10^{-7}	1.5	1.3 × 10^3
SCP	3.2 ± 0.1	1.0 × 10^{-7}	4.3	2.3 × 10^3

[a]Estimated error: 20%.

Table 3. Rate Constants

compound	k_h (s^{-1})	k_{-h} (M^{-1} s^{-1})	k_t (s^{-1})	k_{-t}[a] (s^{-1})	k_i[a] (s^{-1})	k_{-i} (s^{-1})
DOP	0.004	2.3 × 10^4	1.6	0.9	0.09	2.55 × 10^{-4}
GCP	0.013	2.8 × 10^4	1.8	1.2	0.36	2.8 × 10^{-4}
SCP	0.002	2.0 × 10^4	1.3	0.3	0.7	3.1 × 10^{-4}

[a]Estimated error: 20%.

(direct pH jumps). The spectral modifications are compatible with a triprotic acid with pK_a's equal to 3.9, 6.5, and 8.2, Table 1. The absorption spectra of the four species were determined by mathematical decomposition, Figure 1D. The first deprotonation is likely to occur in position 7, a behavior early reported by Jurd and Geissman[16] and confirmed in other anthocyanins.[1] The second deprotonation most probably occurs at position 4 and the third deprotonation at position 5. The pK_a of the first deprotonation compares with 4.1 for the analogue luteolinidin

dx.doi.org/10.1021/jp3110216 | J. Phys. Chem. B 2013, 117, 1901−1910

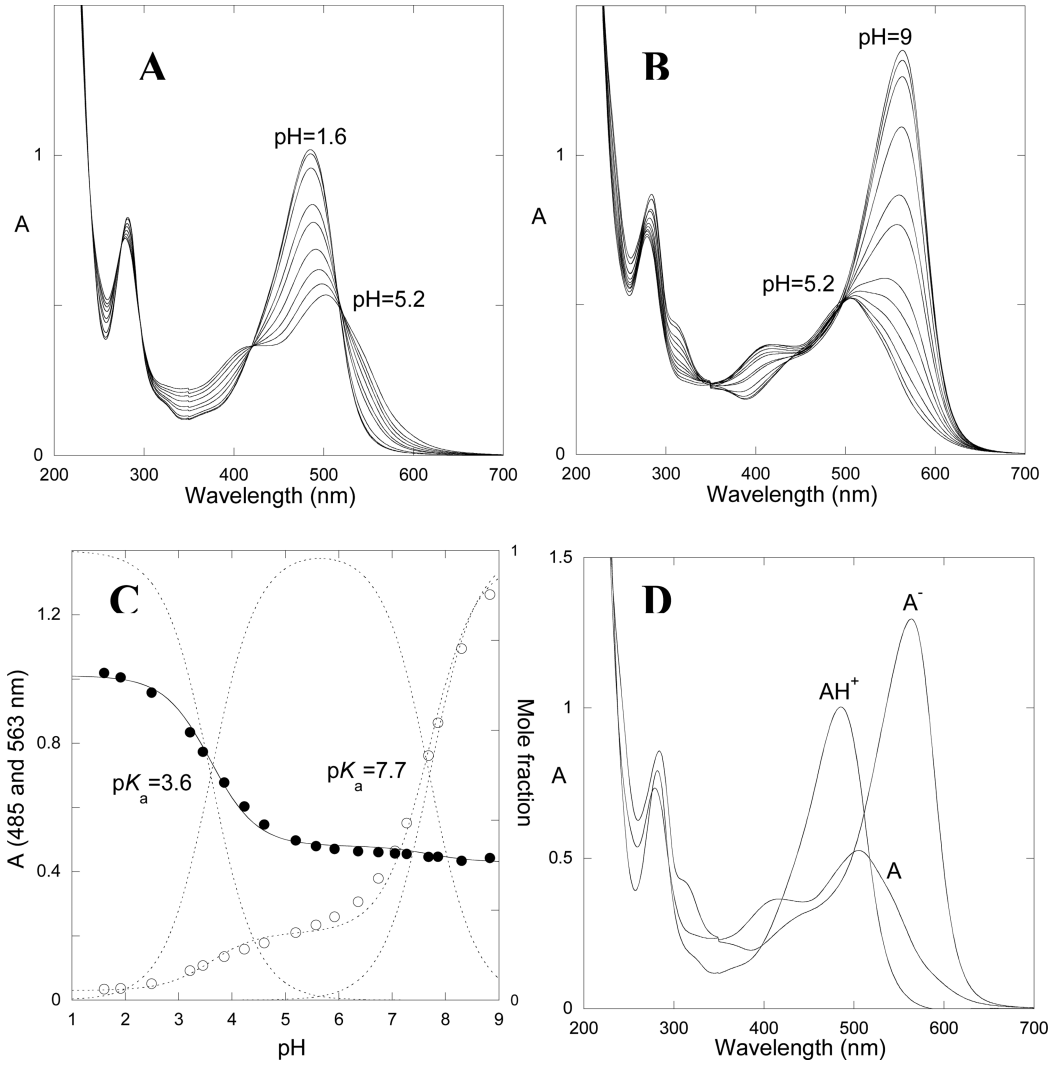

Figure 6. (A) Spectral variations of the compound guaiacylcatechinpyrylium (GCP) 1.6×10^{-4} M (10% EtOH) immediately after a pH jump from 1 to the range 1.6 < pH < 5.2. (B) The same for 5.2 < pH < 9. (C) Fitting of the absorption at 485 and 563 nm as a function of pH. (D) Absorption spectra of the flavylium cation, quinoidal base, and ionized quinoidal base obtained by mathematical decomposition.

(5,7,3′4′-tetrahydroxyflavylium)[17] and 4.2 for apigeninidin (5,7,3′-trihydroxyflavylium).[18]

The pH dependent absorption variations taking place in equilibrated solutions of DOP are represented in Figure 2. The data are compatible with a single acid base equilibrium, eq 1, permitting to define pK'_a = 3.6, a value that compares with 3.8[13] and 4.0,[14] for luteolinidin and apigeninidin. The shape and position of the equilibrium species at moderately acidic medium are compatible with the presence of quinoidal base in equilibrium with *trans*-chalcone. The fraction of the base at the higher pH plateau is given by the ratio K_a/K'_a = 0.5 which is in good agreement with the data of Figure 2.

The relatively large mole fraction of the quinoidal base at the moderately acid equilibrium plateau when compared with anthocyanins (less than 5% in diluted solutions)[1,19] or even 4′,7-dihydroxyflavylium (ca. 10%)[1] was found in the other deoxyanthocyanidins, such as luteolinidin and apigeninidin and in the related compound dragon's blood (4′,7-dihydroxy-5-methoxyflavylium),[20] where the quinoidal base is the major species and the *trans*-chalcone the minor one.

A series of pH jumps from pH 1.0 to higher pH values was carried out, as shown in Figure 3A for the final pH 4.7. The trace taken at 495 nm is compatible with a mole fraction of the base of 0.54 in good agreement with the previous calculations. Representation of the observed rate constants of these pH jumps as a function of pH leads to a bell-shaped curve of Figure 3B.

The bell-shaped curve was previously reported for some flavylium derivatives and presupposes that the equilibrium between B and Cc is much faster than hydration and isomerization. For the present compound, it was not possible to observe the presence of B and Cc through a reverse pH jump (from solutions at higher pH to lower) monitored by stopped flow. As reported previously, the lack of a *cis*−*trans* isomerization barrier allows to apply the steady state approach for the kinetics, that converts Ct into AH^+/A and vice versa, eq 6 and 7.[21−23]

$$\mathbf{Ct} \underset{\frac{K}{1+K_t}k_i}{\overset{k_{-i}}{\rightleftharpoons}} \mathbf{Cc} \rightleftharpoons \mathbf{B} \underset{\frac{[H^+]}{[H^+]+K_a}k_h}{\overset{\frac{k_{-h}}{1+K_t}}{\rightleftharpoons}} \mathbf{AH^+} \rightleftharpoons \mathbf{A} + \mathbf{H^+} \quad (6)$$

$$k_{obs} = \frac{\frac{[H^+]}{[H^+]+K_a}K_hK_tk_i + k_{-i}[H^+]}{\frac{K_tk_i}{k_{-h}} + [H^+]} \quad (7)$$

dx.doi.org/10.1021/jp3110216 | J. Phys. Chem. B 2013, 117, 1901−1910

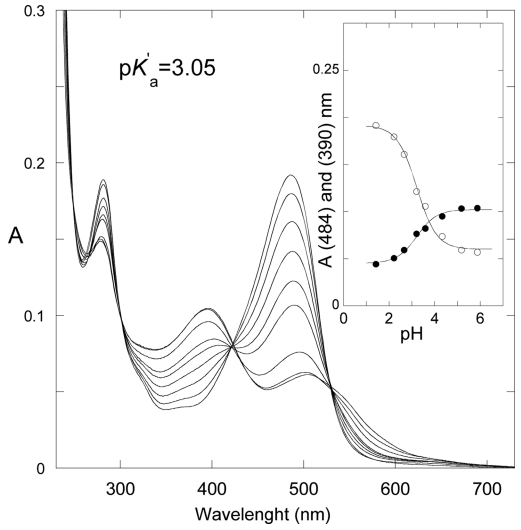

Figure 7. Spectra of equilibrated solutions of GCP (A) at different pH values, showing the equilibrium between AH^+, A, and Ct; inset representation of the fitting obtained at two different wavelengths (pK'_a = 3.05 ± 0.1).

The fitting of eq 7 is represented in Figure 3B and was achieved for pK_a = 3.9; $K_hK_tk_i = 2.6 \times 10^{-8}$; $k_{-i} = 2.55 \times 10^{-4}$ s^{-1}; $k_iK_t/k_{-h} = 6.65 \times 10^{-6}$ M.

Differently from anthocyanins and anthocyanidins, deoxyanthocyanidins exhibit photochemistry and this is a powerful tool to contribute to the assessment of the rate and equilibrium constants of the system, in particular in compounds such as DOP where the reverse pH jumps are unable to detect the kinetic process involving B and Cc.

Figure 4A shows the result of the steady state irradiation of DOP at 366 nm. The spectral variations show the appearance of AH^+/A at the expenses of the Ct disappearance. Flash photolysis, Figure 4B, indicates that upon the flash two parallel processes occur: (i) the forward reaction leading to the formation of flavylium cation, as indicated by the raising of the absorption at 493 nm (Figure 4B up), (ii) the forward reaction that partially recovers Ct, as shown by the recovery of the Ct absorption measured at 393 nm (Figure 4B down). The rate constant measured in both traces is the same as expected for two parallel reactions. The data of the flash photolysis is easily comprehended if an energy level diagram is used (Figure 5, see below how this diagram is obtained). After the flash, Ct disappears to give Cc (which absorbs much less at 393 nm), leading to a bleaching at this wavelength. Cc is not thermodynamically stable and has two ways to disappear, forward to give AH^+/A or backward to recover Ct.

Representation of the rate constant as a function of pH, Figure 4C, can be interpreted considering two regimes: at lower pH values, the hydration is very fast and the tautomerization is the controlling step and the rate constant is given by eq 8.[24,15] At higher pH values, the hydration is the rate determining step, and eq 9 is verified.[25] In eq 8, the rate constant K_{-t}^{OH} corresponds to the basic catalysis of the tautomerization constant,[18] which in DOP is not present at these pH values, and by consequence at low pH values the rate constant is constant.

$$k_{obs(Taut)} = k_i + k_{-t} + k_{-t}^{OH}[OH^-] \quad (8)$$

$$k_{obs(Hyd)} = \frac{k_iK_t}{1 + K_t} + \frac{[H^+]}{[H^+] + K_a}k_h + \frac{k_{-h}[H^+]}{1 + K_t} \quad (9)$$

A global fitting of the data including pK_a, pK'_a, eqs 7−9 leads to the following set of equilibrium and rate constants, Tables 2 and 3.

Other sets of solutions differing slightly from those reported in Tables 2 and 3 are also possible, in particular in which regards the values of the tautomerization constants, due to the lack of its direct calculation from the reverse pH jumps.

The equilibrium constants calculated above permit the drawing of an energy level diagram (Figure 5), which is very useful to the comprehension of the network of chemical reactions, as mentioned above.[1]

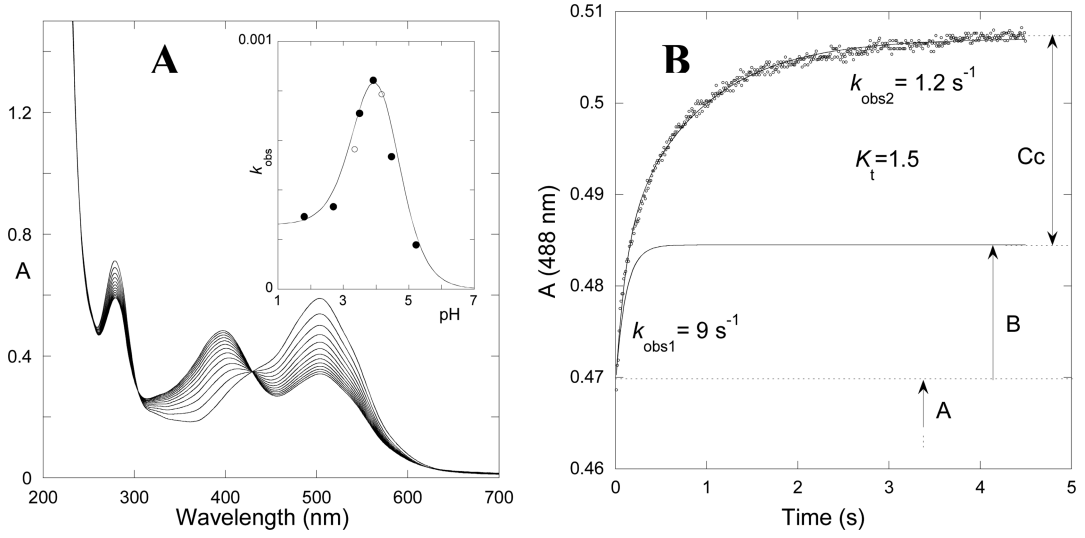

Figure 8. (A) Spectral variations of GCP after a pH jump from 1 to 5.2 ($k_{obs} = 1.8 \times 10^{-4}$ s^{-1}): inset - representation of the observed rate constant as a function of pH. Fitting was achieved for pK_a = 3.6; $K_hK_tk_i = 2.5 \times 10^{-7}$ M^{-1}; $k_{-i} = 0.00028$ s^{-1}; $k_iK_t/k_{-h} = 1.9 \times 10^{-5}$ M. From the ratio $K_hK_tk_i$ / (k_iK_t/k_{-h}), k_h = 0.013 s^{-1}; (●) direct pH jumps; (○) thermal recovery of the photoproduct (see Figure 5). (B) Reverse pH jump from solutions aged about 5 min at pH 5.4 and back to pH 1.2 (K_t = 1.5).

dx.doi.org/10.1021/jp3110216 | J. Phys. Chem. B 2013, 117, 1901−1910

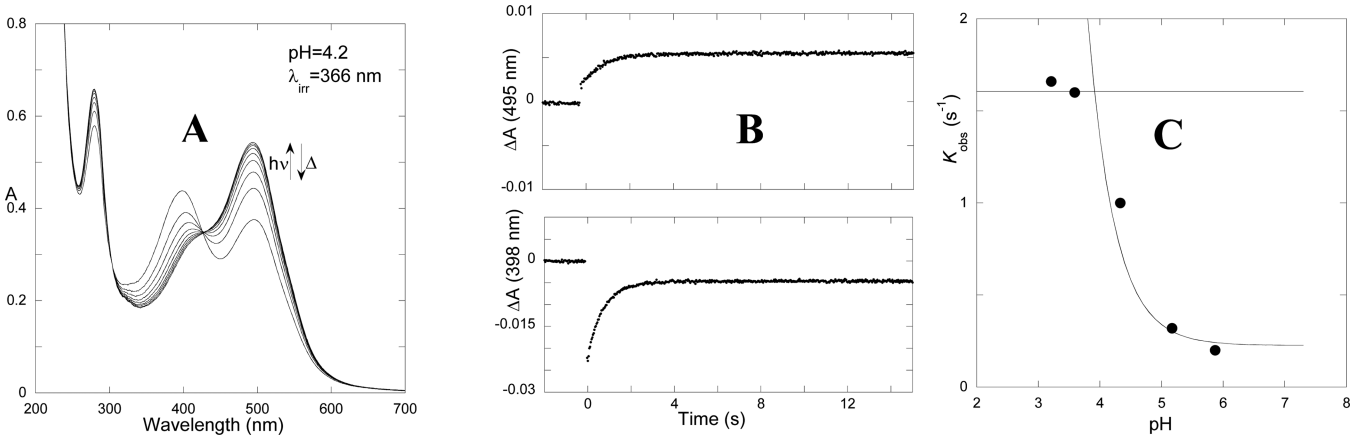

Figure 9. (A) Spectral variations following the irradiation of GCP at pH 4.1 at an irradiation wavelength of 366 nm. (B) Flash photolysis followed at 495 nm (AH^+ and A) up and 398 nm (Ct) bottom. (C) Observed rate constant of the flash photolysis as a function of pH.

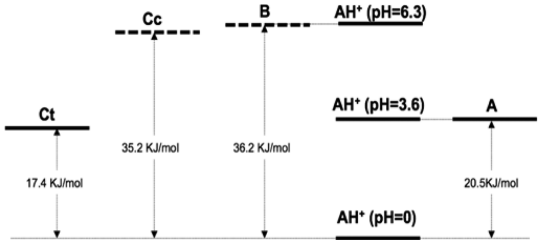

Figure 10. Energy level diagram for GCP based on the equilibrium constants of Table 1.

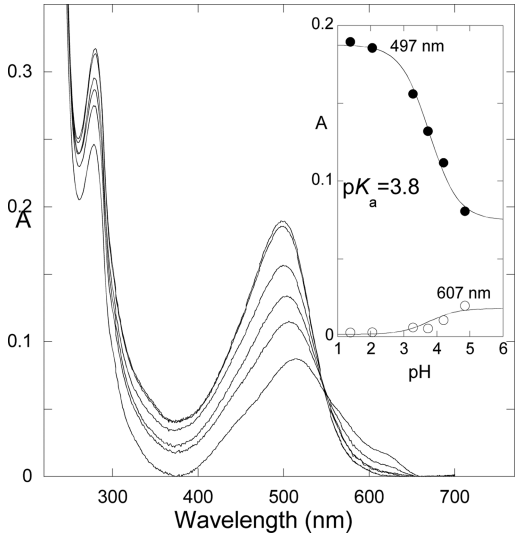

Figure 11. Absorption spectra of solutions of SCP taken immediately after a direct pH jump from stock solutions at pH 1 to higher pH values; inset representation of the fitting obtained at two different wavelengths (pK_a = 3.9 ± 0.1).

2. Guaiacylcathechinpyrylium (GCP). The absorption spectra obtained immediately after a pH jump from equilibrated solutions of GCP 1.6 × 10^{-4} M (10% EtOH) at pH 1.0 to the range 1.6 < pH < 5.2, Figure 6A, and 5.2 < pH < 9, Figure 6B, are compatible with the formation of two quinoidal bases, likely to result from the deprotonation of the flavylium core in position 7 and 4′, Figure 6C. The alternative deprotonation at the catechol substituent is not expected to affect significantly the absorption spectra, as observed in Figure 6B, due to the lack of conjugation with the benzopyrilium ring. The absorption spectra of the species AH^+, A, and A^-, were obtained by mathematical decomposition, Figure 6D.[26]

The solutions of GCP reported in Figure 6 after equilibrium are shown in Figure 7. The shape and position of the absorption spectra are compatible with a pH dependent equilibrium involving the acidic species flavylium cation and a mixture of quinoidal base and *trans*-chalcone at higher pH values, with pK'_a = 3.05. This behavior is very similar to the parent compound DOP, where the equilibrium also involves essentially the same major species, **AH^+**, **A**, and **Ct**.

The kinetic processes from the initial state reported in Figure 6 to the equilibrium, Figure 7, are described in Figure 8A. The spectral changes indicate that at pH 5.2 the quinoidal base initially formed through a pH jump partially disappears to give the *trans*-chalcone. The kinetics follows a monoexponential decay. The rate constants measured at different pH values are reported in the inset of Figure 8A, and follow the previously reported bell-shaped curve. Fitting was achieved for the following parameters $K_hK_tk_i$ = 2.5 × 10^{-7} M^{-1}; k_{-i} = 0.00028 s^{-1}; k_iK_t/k_{-h} = 1.9 × 10^{-5} M. From the ratio $K_hK_tk_i/(k_iK_t/k_{-h})$, k_h = 0.013 s^{-1}.

A first pH jump on stocked solutions at pH 5.14 was carried out, the solutions were kept for 5 min at this pH value, and a reverse pH jump to 1.2 was performed, allowing the monitoring of the flavylium appearance by stopped flow, Figure 8B. The traces indicate that all the quinoidal base present at pH 5.4 was converted during the mixing time of the stopped flow, and the flavylium grows according to a biexponential kinetics. The fast process corresponds to the hydration reaction, which at pH 1.2 is faster than tautomerization due to its proton dependence. The slowest step corresponds to the formation of more flavylium cation from Cc through B, and it is assigned to the rate constant k_{-t} = 1.2.[1] Moreover, from the ratio of amplitudes of both kinetics, the constant K_t = 1.5 was calculated, allowing to obtain k_t = 1.8 and K_hK_i = 8.6 × 10^{-4}.

Similarly to DOP, the compound GCP is photochromic, Figure 9. Irradiation of the *trans*-chalcone leads to the formation of quinoidal base with a quantum yield of 0.1. The system is reversible, and thus, a photostationary state is achieved. The kinetics of the thermal recovery of the photoproduct was measured at two pH values and fits quite well with the bell-shaped curve, Figure 8A. Flash photolysis of equilibrated solutions at pH 4.1 is similar to the parent compound. Within the lifetime of the flash, Ct disappears to give Cc, which goes forward to form AH^+/A or backward to recover Ct. Representation of the observed rate constants from experiments like the one of Figure 9B at different

dx.doi.org/10.1021/jp3110216 | J. Phys. Chem. B 2013, 117, 1901−1910

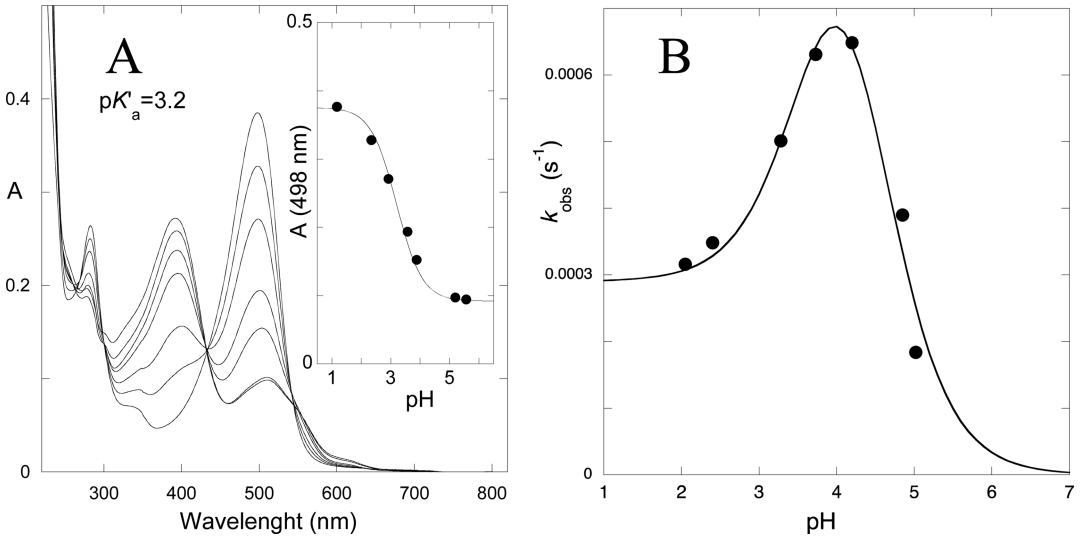

Figure 12. (A) Absorption spectra of equilibrated solutions of SCP. (B) Bell-shaped curve for the compound SCP.

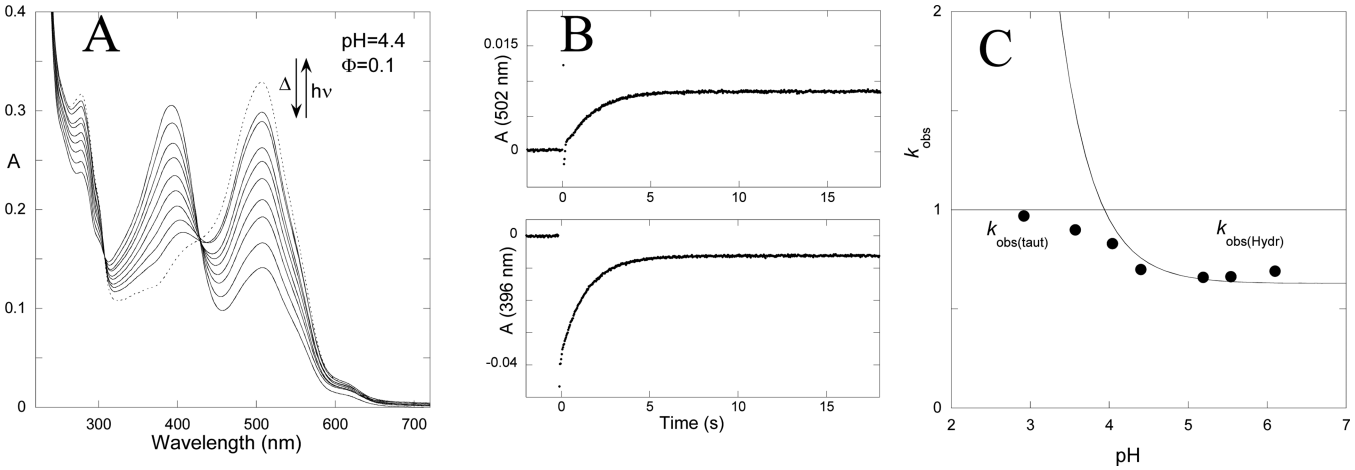

Figure 13. (A) Irradiation of the compound SCP at pH 1.0 (full lines): the spectrum of the solution immediately after its preparation from a pH jump from pH 1.0 to pH 4.4 before being irradiated is also shown (traced line). (B) Flash photolysis traces at 502 nm (AH^+/A) and 396 nm (Ct). (C) Observed rate constant of the flash photolysis as a function of pH.

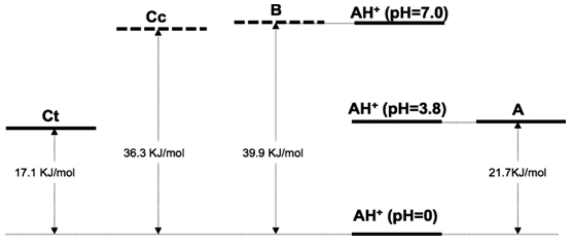

Figure 14. Energy level diagram for SCP based on the equilibrium constants of Table 1. The energy levels of B and Cc were obtained through the fitting of eqs 7–9 due to the lack of observation of traces corresponding to B and Cc in the reverse pH jump experiments carried out by stopped flow.

pH values are shown in Figure 9C. A global fitting was achieved through eqs 8 and 9 and the one of the bell-shaped curve, eq 9 leading to the rate and equilibrium constants presented in Tables 2 and 3.

As in the case of DOP, it is easy to construct an energy level diagram where the five species are relatively positioned, Figure 10. It is worth noting the fact that similarly to DOP (and to SCP, see below) the energy level of Ct and A are close and lower relatively to B and Cc, as expected from the shape and position of the absorption spectra at the equilibrium.

3. Syringylcatechinpyrylium (SCP). The absorption spectra of SCP were obtained immediately after the pH jump, and a value of pK_{a1} = 3.8 was obtained in Figure 11.

The further ionization constants were not determined due to the appearance of some decomposition which can be attributed to the presence of the cathecol unit, which is known to be easily oxidized at higher pH values. The absorption spectra of the equilibrated solutions, Figure 12, are again compatible with an equilibrium involving essentially the species AH^+, A, and Ct.

The spectral variations upon irradiation of SCP of equilibrated solutions at pH 4.4 are shown in Figure 13, and it can be concluded that SCP shows a behavior similar to DOP and GCP. However, there are some differences which can be easily visualized from the data of Figures 4C, 9C, and 13C. Inspection of eq 9 used to fit the data indicates that it tends to eq 10 when the proton concentration decreases.

$$k_{obs(hydr)} = \frac{k_i K_t}{1 + K_t} \qquad (10)$$

dx.doi.org/10.1021/jp3110216 | J. Phys. Chem. B 2013, 117, 1901–1910

The value of eq 10 defines the plateau reached in the above-mentioned figures, respectively 0.057, 0.22, and 0.63. This is also in accordance with the data reported in Tables 1 and 2.

Flash photolysis of equilibrated solutions at pH 4.4 is similar to the parent compound and GCP. Within the lifetime of the flash, Ct disappears to give Cc, which goes forward to form AH^+/A or backward to recover Ct. Representation of the observed rate constants from experiments like the one of Figure 13B at different pH values is shown in Figure 13C.

The energy level diagram of SCP is shown in Figure 14 and is qualitatively similar to DOP and GCP, showing the higher stability of the species A and Ct at higher pH values, much higher than B and Cc.

CONCLUSION

The network of chemical reactions involving anthocyanins and related compounds is pH dependent, and by consequence, the detailed kinetics of the system have been obtained through pH jumps, which allow us to follow the relaxation processes toward the new equilibrium. When the flavylium derived networks of chemical reactions exhibit photochemistry, flash photolysis is an excellent complementary technique to collect kinetic information on the system without changing the pH. This is particularly important for flavylium derivatives possessing a low *cis*−*trans* isomerization barrier, since hemiketal, B, and *cis*-chalcone, Cc, are transient species not detected from the pH jump studies. In fact, when compared to common wine anthocyanins in which B (incolor) is the major species at higher pH values, sometimes at the pH of the wine, these oaklin compounds have a behavior more similar to simpler deoxyanthocyanidins, in which the equilibrium involves essentially AH^+, A, and Ct and the mole fraction of the quinoidal base A is approximately 50%. Furthermore, the pK'_a values obtained for GCP and SCP (3.05 and 3.2, respectively) are higher than the ones reported for malvidin-3-glucoside (2.54[5] and 2.3[27]), meaning that the flavylium cation is more stable in the former. The lost of color in solution is thereby greatly diminished in oaklin compounds when compared to other anthocyanins, not only because the pK'_a is greater but also because the mole fraction of the base is substantially higher at higher pH values. In consequence, oaklins which are formed through the reaction of catechin and oak wood aldehydes may play an important role in some color changes observed in wine aging and may contribute to the overall color presented by some wines. Nevertheless, it is important to note that anthocyanins like malvidin-3-glucoside are still present in wines at concentration levels far higher than oaklins and their contribution to wine color must not be underestimated, neither the effects of copigmentation.[28]

Despite some differences, the general behavior of guaiacylcatechinpyrylium and syringylcatechinpyrylium is quite similar to the model compound deoxypeonidin. Given the fact that the loss of color in solution of these compounds is lower than anthocyanins, they may be regarded as potential commercial food colorants. However, further studies should be performed in order to test their stability to other conditions (temperature, sulfites, etc.) as well as to study their antioxidant properties.

AUTHOR INFORMATION

Notes

The authors declare no competing financial interest.

ACKNOWLEDGMENTS

The authors thank FCT (Fundação para a Ciência e Tecnologia) for a PhD grant (ref SFRH/BD/68736/2010) and a research grant (PTDC/QUI-QUI/117996/2010). This research was also supported by a research project grant (PTDC/QUI-QUI/117996/2010) funded by FCT (Fundação para a Ciência e Tecnologia).

REFERENCES

(1) Pina, F.; Melo, M. J.; Laia, C. A. T.; Parola, A. J.; Lima, J. C. Chemistry and Applications of Flavylium Compounds: a Handful of Colours. *Chem. Soc. Rev.* **2012**, *41*, 86A−908.

(2) Kumpulainen, J. T.; Salonen, J. T. *Natural Antioxidants and Food Quality in Atherosclerosis and Cancer Prevention*, The Royal Society of Chemistry: Cambridge, U.K., 1996.

(3) Brouillard, R.; Dubois, J.-E. Mechanism of the Structural Transformations of Anthocyanins in Aqueous Media. *J. Am. Chem. Soc.* **1977**, *99*, 1359−1364.

(4) Brouillard, R.; Delaporte, B. Chemistry of Anthocyanin Pigments. 2. Kinetic and Thermodynamic Study of Proton Transfer, Hydration, and Tautomeric Reactions of Malvidin 3-glucoside. *J. Am. Chem. Soc.* **1977**, *99*, 8461−8468.

(5) Brouillard, R.; Delaporte, B.; Dubois, J.-E. Chemistry of Anthocyanin Pigments. 3. Relaxation Amplitudes in pH Jump Experiments. *J. Am. Chem. Soc.* **1978**, *100*, 6202−6205.

(6) Pina, F. Thermodynamics and Kinetics of Flavylium Salts Malvin Revisited. *J. Chem. Soc., Faraday Trans.* **1998**, *94*, 2109−2116, 3781−3781.

(7) Brouillard, R.; Lang, J. The Hemiacetal−cis-Chalcone Equilibrium of Malvin, a Natural Anthocyanin. *Can. J. Chem.* **1990**, *68*, 755−761.

(8) Pina, F.; Melo, M. J.; Parola, A. J.; Maestri, M.; Balzani, V. pH-Controlled Photochromism of Hydroxyflavylium Ions. *Chem.—Eur. J.* **1998**, *4*, 2001−2007.

(9) Freitas, V.; Sousa, C.; Silva, A. M. S.; Santos-Buelga, C.; Mateus, N. Synthesis of a New Catechin-pyrylium Derived Pigment. *Tetrahedron Lett.* **2004**, *45*, 9349−9352.

(10) Sousa, C.; Mateus, N.; Perez-Alonso, J.; Santos-Buelga, C.; Freitas, V. Preliminary Study of Oaklins, a New Class of Brick-red Catechinpyrylium Pigments Resulting from the Reaction between Catechin and Wood Aldehydes. *J. Agric. Food Chem.* **2005**, *53*, 9249−9256.

(11) Iacobucci, G. A.; Sweeny, J. G. The Chemistry of Anthocyanins, Anthocyanidins and Related Flavylium Salts. *Tetrahedron* **1983**, *39*, 3005−3038.

(12) Khalil, A.; Baltenweck-Guyot, R.; Ocampo-Torres, R.; Albrecht, P. A Novel Symmetrical Pyrano-3-deoxyanthocyanidin from a Sorghum Species. *Phytochem. Lett.* **2010**, *3*, 93−95.

(13) Dangles, O.; Elhajji, H. Synthesis of 3-Methoxy- and 3-(β-D-Glucopyranosyloxy)flavylium Ions. Influence of the Flavylium Substitution Pattern on the Reactivity of Anthocyanins in Aqueous Solution. *Helv. Chim. Acta* **1994**, *77*, 1595−1610.

(14) Sousa, A.; Mateus, N.; Freitas, V. A Novel Reaction Mechanism for the Formation of Deoxyanthocyanidins. *Tetrahedron Lett.* **2012**, *53*, 1300−1303.

(15) Pina, F.; Melo, M. J.; Ballardini, R.; Flamigni, L.; Maestri, M. Micelle Effect on Ground and Excited State Proton Transfer Reactions Involving the 4-Methyl-7-hydroxyflavylium Cation. *New J. Chem.* **1997**, *21*, 969−976.

(16) Jurd, L.; Geissman, T. A. Anthocyanins and Related Compounds. II. Structural Transformations of Some Anhydro Bases. *J. Org. Chem.* **1963**, *28*, 2394−2397.

(17) Melo, M. J.; Moura, S.; Roque, A.; Maestri, M.; Pina, F. Photochemistry of Luteolinidin - "Write-lock-read-unlock-erase" with a Natural Compound. *J. Photochem. Photobiol., A* **2000**, *135*, 33−39.

(18) Brouillard, R.; Iacobucci, G. A.; Sweeny, J. G. Chemistry of Anthocyanin Pigments 0.9. UV-Visible Spectrophotometric Determination of the Acidity Constants of Apigeninidin and 3 Related 3-Deoxyflavylium Salts. *J. Am. Chem. Soc.* **1982**, *104*, 7585−7590.

(19) Leydet, Y.; Gavara, R.; Petrov, V.; Diniz, A. M.; Parola, A. J.; Lima, J. C.; Pina, F. A Flash Photolysis and Stopped-Flow

Spectroscopy Study of 3′,4′-Dihydroxy-7-O-β-D-glucopyranosyloxyflavylium Chloride, an Anthocyanin Analogue Exhibiting Efficient Photochromic Properties. *Phytochemistry* **2012**, *244*, 54−64.
(20) Melo, M. J.; Sousa, M.; Parola, A. J.; Melo, J. S.; Catarino, F.; Marçalo, J.; Pina, F. Identification of 7,4′-Dihydroxy-5-methoxyflavylium in "Dragon's Blood": To Be or Not To Be an Anthocyanin. *Chem.—Eur. J.* **2007**, *13*, 1417−1422.
(21) Pina, F.; Petrov, V.; Laia, C. A. T. Photochromism of Flavylium Systems. An Overview of a Versatile Multistate System. *Dyes Pigm.* **2012**, *92*, 877−889.
(22) Petrov, V.; Pina, F. Analytical Resolution of the Reaction Rates of Flavylium Network by Laplace Transform. *J. Math. Chem.* **2010**, *47*, 1005−1026.
(23) Pina, F.; Melo, M. J.; Parola, A. J.; Maestri, M.; Balzani, V. pH-Controlled Photochromism of Hydroxyflavylium Ions. *Chem.—Eur. J.* **1998**, *4*, 2001−2007.
(24) McClelland, R. A.; Gedge, S. Hydration of the Flavylium Ion. *J. Am. Chem. Soc.* **1980**, *102*, 5838−5848.
(25) Gago, S.; Petrov, V.; Parola, A. J.; Pina, F. Synthesis, Characterization and Photochromism of 3′-Butoxyflavylium Derivatives. *J. Photochem. Photobiol., A* **2012**, *244*, 54−64.
(26) Antonov, L.; Petrov, V. Quantitative Analysis of Undefined Mixtures - "Fishing Net" Algorithm. *Anal. Bioanal. Chem.* **2002**, *374*, 1312−1317.
(27) Nave, F.; Petrov, V.; Pina, F.; Teixeira, N.; Mateus, N.; Freitas, V. Thermodynamic and Kinetic Properties of a Red Wine Pigment: Catechin-(4,8)-Malvidin-3-O-glucoside. *J. Phys. Chem. B* **2010**, *114*, 13487−13496.
(28) Boulton, R. The Copigmentation of Anthocyanins and Its Role in the Color of Red Wine: a Critical Review. *Am. J. Enol. Vitic.* **2001**, *52*, 67−87.